HHS Public Access

Author manuscript

Anal Chem. Author manuscript; available in PMC 2023 July 10.

Published in final edited form as:

Anal Chem. 2023 July 04; 95(26): 9746–9753. doi:10.1021/acs.analchem.2c05731.

DiLeu isobaric labeling coupled with limited proteolysis mass spectrometry for high-throughput profiling of protein structural changes in Alzheimer's disease

Haiyan Lu[1], **Bin Wang**[1], **Yuan Liu**[1], **Danqing Wang**[2], **Lauren Fields**[2], **Hua Zhang**[1], **Miyang Li**[2], **Xudong Shi**[3], **Henrik Zetterberg**[4,5,6,7,8], **Lingjun Li**[1,2,9,*]

[1]School of Pharmacy, University of Wisconsin-Madison, Madison, WI, 53705, USA

[2]Department of Chemistry, University of Wisconsin-Madison, Madison, WI, 53706, USA

[3]Division of Otolaryngology, Department of Surgery, School of Medicine and Public Health, University of Wisconsin-Madison, Madison, WI, 53792, USA

[4]Institute of Neuroscience and Physiology, Sahlgrenska Academy, University of Gothenburg, 43141, Gothenburg, Sweden

[5]Clinical Neurochemistry Laboratory, Sahlgrenska University Hospital, Mölndal, 43130, Sweden

[6]Department of Molecular Neuroscience, UCL Institute of Neurology, London, WC1N 3BG, UK

[7]UK Dementia Research Institute at UCL, London, WC1N 3BG, UK

[8]Hong Kong Center for Neurodegenerative Diseases, Clear Water Bay, Hong Kong, 999077, China

[9]Lachman Institute for Pharmaceutical Development, School of Pharmacy, University of Wisconsin-Madison, Madison, WI 53705, USA

Abstract

High-throughput quantitative analysis of protein conformational changes has a profound impact on our understanding of the pathological mechanisms of Alzheimer's disease (AD). To establish an effective workflow enabling quantitative analysis of changes in protein conformation within multiple samples simultaneously, here we report the combination of *N,N*-dimethyl leucine (DiLeu) isobaric tag labeling with limited-proteolysis mass spectrometry (DiLeu-LiP-MS) for high-throughput structural protein quantitation in serum samples collected from AD patients and control donors. 23 proteins were discovered to undergo structural changes, mapping to 35 unique

[*]**Corresponding author**: lingjun.li@wisc.edu. Phone: +1-608-265-8491; Fax: +1-608-262-5345.

Conflicts of interest

Henrik Z. has served at scientific advisory boards and/or as a consultant for Abbvie, Alector, ALZPath, Annexon, Apellis, Artery Therapeutics, AZTherapies, CogRx, Denali, Eisai, Nervgen, Novo Nordisk, Passage Bio, Pinteon Therapeutics, Red Abbey Labs, reMYND, Roche, Samumed, Siemens Healthineers, Triplet Therapeutics, and Wave, has given lectures in symposia sponsored by Cellectricon, Fujirebio, Alzecure, Biogen, and Roche, and is a co-founder of Brain Biomarker Solutions in Gothenburg AB (BBS), which is a part of the GU Ventures Incubator Program (outside submitted work).

Supporting information

Additional information as noted in text. This material is available free of charge via the Internet at http://pubs.acs.org.
Additional experimental details, materials, methods, as well as figures and tables of experimental result (DOC).

conformotypic peptides with significant changes between the AD group and the control group. 7 out of 23 proteins, including CO3, CO9, C4BPA, APOA1, APOA4, C1R and APOA, exhibited potential correlation with AD. Moreover, we found that complement proteins (e.g., CO3, CO9 and C4BPA) related to AD exhibited elevated levels in the AD group compared to those in the control group. These results provide evidence that the established DiLeu-LiP-MS method can be used for high-throughput structural protein quantitation, which also showed great potential in achieving large-scale and in-depth quantitative analysis of protein conformational changes in other biological systems.

Graphical Abstract

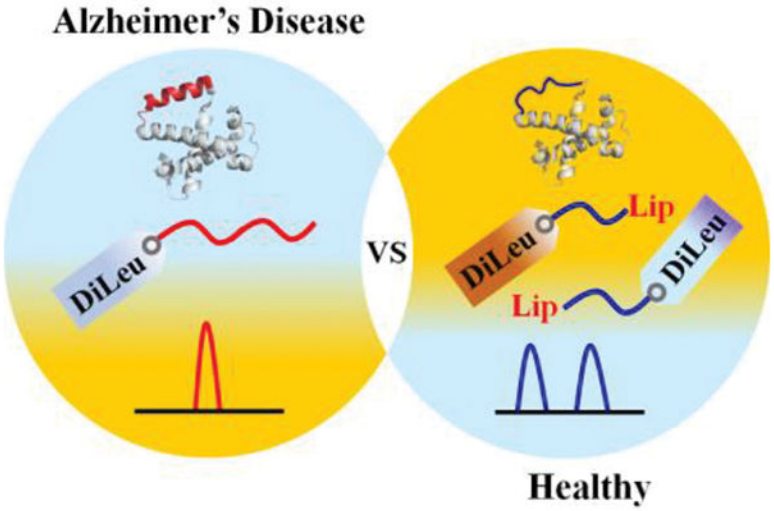

Keywords

DiLeu isobaric labeling; limited proteolysis mass spectrometry; high-throughput protein quantitation; structural protein quantitation; Alzheimer's disease

INTRODUCTION

Changes in protein conformation induced by external disturbances or internal cues can negatively affect protein activity, leading to various human diseases, such as Alzheimer's, Parkinson's, and Huntington's diseases.[1–3] Particularly, in amyloidosis and other neurodegenerative diseases, protein conformation change increases propensity to form insoluble plaques and amyloid fibrils.[4] As a typical protein aggregation disease, Alzheimer's disease (AD) is featured by neuropathological hallmarks, including neurofibrillary tangles (NFTs) and senile plaques.[5–8] NFTs are intraneuronal aggregates of hyperphosphorylated tau, while senile plaques mainly composed of amyloid β-peptide (Aβ) deposits in extracellular space.[9] Despite extensive studies focused on tau phosphorylation[10, 11] and Aβ aggregation,[12, 13] the system-wide analysis of protein conformational changes in AD has received much less attention. This is partly due to the lack of methods to systematically probe protein structural changes in complex biological samples. Therefore, the development of a method for capturing protein structural transitions both in complex AD

biological samples (e.g., serum) and on a large scale would have a profound impact on our understanding of the pathological mechanisms of AD.

Available approaches for protein structural studies include X-ray crystallography, nuclear magnetic resonance (NMR),[14] Förster resonance energy transfer (FRET)[15] and in-cell NMR.[16] Despite tremendous advances in these technologies, these methods are not suitable for studying large scale protein conformation changes in complex biological samples. Limited proteolysis-coupled mass spectrometry (LiP-MS) is a useful technique for probing protein structural changes in complex biological samples on a large scale and has found successful applications in multiple systems, such as protein thermal unfolding,[17] and drug-protein interactions.[2, 18] LiP-MS is not inherently high-throughput, as it is limited to only one sample in a single liquid chromatography-mass spectrometry (LC-MS) run. To enable high-throughput analysis in a single LC-MS run, mass spectrometry (MS)-based isobaric labeling techniques such as amino acid-coded mass tags (AACT),[19] tandem mass tags (TMTs),[20] isobaric tags for relative and absolute quantitation (iTRAQ),[21] and *N,N*-dimethyl leucine (DiLeu)[22, 23] isobaric tagging have been widely used in quantitative proteomics studies, with the advantages of increased analytical throughput, improved quantitation accuracy, and reduced run-to-run variability within biological or technical replicates. Here, we hypothesize that the combination of DiLeu isobaric labeling with LiP-MS will enable high-throughput structural protein quantitation and provide a better understanding of the protein structure-function relationships.

In this study, we developed a workflow combining DiLeu isobaric tag labeling with LiP-MS (DiLeu-LiP-MS) to perform high-throughput structural protein quantitation in AD serum samples. The feasibility of DiLeu-LiP-MS was initially validated through the holomyoglobin and apomyoglobin model systems. Upon demonstration of proof-of-concept results, the DiLeu-LiP-MS method was employed for AD serum sample analysis. This method resulted in the identification of 7 proteins, including CO3, CO9, C4BPA, APOA1, APOA4, C1R and APOA, which were determined to undergo specific regional structural changes and exhibited a potential relationship with AD. Moreover, our results suggested that several complement proteins, including CO3, CO9 and C4BPA, related to documented AD pathways, and exhibited higher levels in the AD group compared with that in the control group. These results provide evidence that our DiLeu-LiP-MS method has great potential to achieve large-scale and in-depth quantitative analysis of structural changes of proteins in other biological systems.

EXPERIMENTAL SECTION

Serum Protein Extraction and Limited Proteolysis

Details for human serum samples and chemical reagents involved in this study are included in the Supporting Information. Protein concentration in each serum sample was adjusted by native lysis buffer (20 mM HEPES buffer, 150 mM KCl, 10 mM $CaCl_2$) containing Roche Mini cOmplete Protease Inhibitor Cocktail (EDTA-free) at pH of 7.5. After protein concentration assay using a bicinchoninic acid (BCA) kit, 400 μg serum protein from AD patients or controls were evenly divided into 2 aliquots for LiP samples and trypsin samples, respectively. The broad-specificity proteinase K (PK) was added to the LiP samples at an

enzyme/substrate (E:S) ratio of 1:100 (w/w) and incubated for 5 min at room temperature (RT), while the same volume of water was added to the trypsin samples. The digestion was quenched by transferring the reaction mixture to a tube containing guanidine hydrochloride to a final concentration of 7.4 M and then boiled for 3 min. It should be noted that the water bath must be >95 °C to irreversibly inactivate the PK enzyme.[3] The protein mixtures were then subjected to complete tryptic digestion after cooled at RT for 5 min, and desalted peptides were used for DiLeu labeling. To improve proteome coverage and strengthen detection of low-abundance proteins, off-line high pH (HpH) fractionation was conducted prior to liquid chromatography-tandem mass spectrometry (LC-MS/MS) analysis. For details about tryptic digestion, DiLeu labeling, as well as HpH fractionation and LC-MS/MS refer to Supporting Information. The detailed workflow of DiLeu-LiP-MS is shown in Figure 1.

Data Analysis

The details of database search refer to Supporting Information. Reporter ion intensities among three sets and across channels in each set were normalized through sum of total intensity of shared sample. After normalization by shared sample, only LiP peptides data corresponding to unique proteins were selected to perform normalization analysis, which was normalized by using protein abundance changes in trypsin samples as a normalization factor to correct for changes in protein abundance and possible intracellular proteolytic activity. Different protein isoforms can introduce ambiguity when protein quantification is conducted at the peptide level. Thus, it is meaningful to perform normalization of LiP-MS peptide data by matching PK/trypsin-digested peptides with trypsin-digested peptides, accounting for overlapped sequences. Missing intensities were replaced using the function of “replace missing values from normal distribution” in Perseus (Version1.6.15.0) prior to further analysis. Two-sample Student’s *t*-test with a two-tailed distribution was conducted using Perseus for screening of significantly changed proteins and peptides between AD and control serum samples. The p-value is subjected to permutation-based FDR for multiple testing correction. Peptide and protein intensity profiling as well as box plots were obtained through Origin 2020. Relative quantitation of peptide abundances in label-free LiP-MS experiment was performed using Skyline. Visualization of protein structure was downloaded from the Protein Data Bank (PDB) (https://www.rcsb.org/) and loaded into PyMOL (2.5.2). Functional classification analysis and pathway enrichments analysis were conducted through Panther (http://www.pantherdb.org/) and DAVID (https://david.ncifcrf.gov/home.jsp), respectively. The mass spectrometry proteomics data have been deposited in ProteomeXchange, which can be obtained via Mass Spectrometry Interactive Virtual Environment (MassIVE) accession MSV000091408 and PRoteomics IDEntifications database (PRIDE) accession PXD040585.

Results and Discussion

Evaluating the performance of DiLeu-LiP-MS for quantitative analysis of protein structural changes

Holomyoglobin and apomyoglobin model systems were utilized as initial tests for label-free LiP-MS experiment to validate the feasibility of DiLeu-LiP-MS in quantitative analysis of

protein structural changes. Details of apomyoglobin preparation from holomyoglobin by 2-butanone extraction refers to Supporting Information. As shown in Figure 2, we found that the intensity of fully tryptic peptide (GHHEAELKPLAQSHATK) in holomyoglobin (Figure 2A) was significantly higher (~141-fold change) than that of apomyoglobin (Figure 2E) for LiP-MS group and showed comparable level in holomyoglobin (Figure 2B) and apomyoglobin (Figure 2F) for trypsin group, while two half-tryptic peptides (GHHEAELKPL and GHHEAELKPLAQ) detected in holomyoglobin (Figures 2C and 2D) were significantly lower than that of apomyoglobin (Figures 2G and 2H) in LiP-MS group. We propose that the fully tryptic peptide (GHHEAELKPLAQSHATK) in apomyoglobin was selectively cleaved, whereas in holomyoglobin it was consistently protected from proteolytic cleavage, resulting in two half-tryptic peptides (GHHEAELKPL and GHHEAELKPLAQ) displayed inverse abundance changes between apomyoglobin and holomyoglobin. These results were supported by previous structural studies of myoglobin via LiP-MS[2] and other methods. For example, top-down hydrogen/deuterium exchange (HDX) indicated that extensive deuteration takes place at the intervening loops and in the F-region,[24] and fast photochemical oxidation of proteins (FPOP) strategy revealed that helix F has the higher accessibility among all apomyoglobin peptides.[25] In addition, fast fluoroalkylation of proteins (FFAP) strategy revealed that the increased modification of aromatic amino acids situated at helix F was observed in apomyoglobin.[26] Overall, this leads us to conclude that the region helix F encompassing fully tryptic peptides, GHHEAELKPLAQSHATK, is readily accessible for PK and is more flexible in apomyoglobin. Typically, chromatographic retention time should be a constant for a given analyte at specific mobile phase composition, stationary phase, temperature, and pH,[27] but non-linear retention time shifts in chromatograms across multiple sample runs are often observed.[28] Herein, retention time shifts for the peptides including GHHEAELKPL and GHHEAELKPLAQ in holomyoglobin and apomyoglobin were observed. In our method, the flow rate and composition of mobile phase as well as integration are exactly the same, so the primary causative factor of retention time shifts is column temperature during the run, as small variations in the column temperature can have a significant effect on the retention time.[29]

To assess the reproducibility of data, we calculated the coefficient of variation (CV) among different measurements and showed in the tables for confidently identified peptides of holomyoglobin and apomyoglobin in the LiP-MS group (Table S2) and the trypsin group (Table S3). It is observed from Table S3 that the intensity of peptide (MGLSDGEWQQVLNVWGK) (1–17) is displayed as 0 compared to peptide (GLSDGEWQQVLNVWGK) (2–17) in apomyoglobin. This result might be related to the low signal intensity of peptide (MGLSDGEWQQVLNVWGK) (1–17) in apomyoglobin, as the principle of the LFQ algorithm in MaxQuant is MS1-based, calculating the integration of each peptide signal from the LC-MS chromatography.[30, 31] If the peptide signal intensity used for protein quantification is too low in sample, it leads to a situation where the peak area integral quantification has no value, and thus the intensity in that sample is reported as 0. Also, our results showed that half-tryptic peptides, including GLSDGEWQ (2–9) and GLSDGEWQQVLN (2–13), have significantly higher intensities in apomyoglobin than that of holomyoglobin for LiP-MS group (Table S2). Furthermore, their fully tryptic peptide GLSDGEWQQVLNVWGK (2–17) has comparable intensity

levels in holomyoglobin and apomyoglobin in the trypsin group (Table S3). Since fully tryptic peptide GLSDGEWQQVLNVWGK (2–17) is in helix A, together these findings indicate that helix A has solvent accessibility, in line with the phenomenon that has been documented by HDX, FPOP and FFAP. For example, HDX revealed that the helix A is only marginally developed with deuteration levels around 0.8,[24] and FPOP data showed that protein segment (GLSDGEWQQVLNVWGK) (2–17) located on helix A gains different levels of protection with respect to folding time,[25] and modification on helix A was also observed by FFAP.[26] Overall, each method can provide insight of unique features of surface accessibility and flexibility.[32] Since experimental conditions (e.g., pH, temperature, solvent additives) affect the results obtained across different methods, the differences in modification sites observed between LiP-MS and HDX/FPOP/FFAP further highlight the necessity of exact experimental conditions to enable comparison analysis of conformational changes implicated in specific protein regions across different techniques.

Based on the above satisfactory results of label-free LiP-MS quantitation, the quantitative accuracy and dynamic range of 8-plex DiLeu-LiP-MS for high-throughput quantitation of protein structural changes were further evaluated. As shown in Figure 3, we observed that the median DiLeu ratios obtained by all quantified peptides were 0.98:1.02:0.96:1.03:0.95:0.96 in the 1:1:1:1:1:1:1:1 ratio sample, and 2.11:5.69:10.08:10.91:4.98:2.03 in the 1:2:5:10:10:5:2:1 ratio sample, which were consistent with theoretical ratios across all channels. These results demonstrated that 8-plex DiLeu-LiP-MS could be used for high-throughput quantitation of protein structural changes across a usable dynamic range. It should be noted that because DiLeu tag labeling was performed at the peptide level, formation of a new peptide bond was achieved through an amine reactive group (triazine ester) targeting the N-terminus and ε-amino group of the lysine side chain of the peptide.[33] As such, modification of heme by DiLeu tag labeling could not occur.

Relative quantitation of conformotypic peptides in AD and control serum samples

We sought to assess whether the established DiLeu-LiP-MS method would be amenable to unbiased identification of proteins that underwent structural changes between AD and control serum samples. A total of resulting 30 samples (21 serum samples including 11 AD and 10 control serum samples, three sets of 8-plex DiLeu tags were used to label 21 serum samples, each set obtained 5 combined fractions after HpH fractionation, each combined fractionation included PK treatment and trypsin-only treatment samples) were analyzed by LC-MS/MS on a high-resolution Orbitrap Fusion Lumos mass spectrometer. A total of 2023 peptides and 161 proteins were identified in the LiP samples, and 2104 peptides and 240 proteins were identified in trypsin digested samples (protein false discovery rate (FDR) ~1%) (Figure S1). The numbers of identified peptides in LiP samples was 4% fewer than in trypsin samples, a finding that was consistent with previous report, where it is expected that the total number of peptides identified in LiP samples should be approximately 25% fewer than that of the trypsin sample.[3] Among the 2023 peptides identified in LiP samples, 1277 unique peptides were selected for further analysis. To identify LiP cleavage sites, unique peptides with an abundance difference (p-value <0.05), were focused after corrections for changes in protein abundance and possible intracellular proteolytic activity. This filtering criteria led to the identification of 35 unique peptides corresponding to 23 proteins. By

comparing PK-treated to trypsin treated samples, these 35 peptides were used to identify their corresponding protein region undergoing structural changes.

As noted in Figures 4A and 4B, some fully tryptic peptides have more than one LiP cleavage site. Relative quantitation results indicated that half-tryptic peptides derived from cleavage within fully tryptic peptides with more than one cleavage site showed significant changes between the AD group and the control group, and they also showed increased levels in AD group compared to that in the control group (Figure S2). Theoretically, fully tryptic peptides and half-tryptic peptides in LiP samples should display inverse abundance change trends, and the abundance of fully tryptic peptides embedding LiP sites in trypsin samples is expected to be higher than that of the LiP samples.[2, 3] We found abundance change trends of fully tryptic peptides and their half-tryptic peptides detected in our experiment agree well with these principles. For example, 11 fully tryptic peptides were only detected in the trypsin samples, while their half-tryptic peptides were only detected in the LiP samples (Figures 4C, 4D, and Figure S3). The readout of a LiP-MS experiment is affected by the digestion efficiency of PK, as well as a range of molecular events, including diverse interactions with other proteins or bioactive molecules, such as DNA, RNA, ligands, and metabolites, as well as post-translational modifications (PTMs).[34] These properties, equipped to alter the structure of the protein, can also influence digestion efficiency of PK. In principle, flexible and accessible regions (such as loops or unstructured domains) of a protein are much more susceptible to the time-limited digestion by PK, in comparison to folded or aggregated regions.[35] Therefore, the alteration of PK digestion efficiency can provide context of structural flexibility and accessibility.

LiP samples are not suitable for the estimation of protein abundance changes across different conditions because the result of a large portion of tryptic peptides will embed structure-specific cleavages.[3] Thus, samples subjected to trypsin-only treatment were used for the relative quantitation of protein abundance changes. Here, 23 proteins underwent structural changes in trypsin group were subjected to relative quantitation (Figure S4). It could be found from Figure S4 that only two proteins (including FA12 and CBPN) showed significant changes between the AD group and the control group. Additionally, 4 proteins (including IGKC, IGHG3, APOA2, and APOA) showed decreased levels in the AD group compared to the control group, and 6 proteins (including IGHG4, AMBP, APOB, APOA4, PROS, and CFAH) showed similar levels between the AD group and the control group, whereas all conformotypic peptides in the LiP group showed significant changes between the AD and the control serum samples and were upregulated in the AD group (Figures 4C, 4D, S2, and S3). These results indicated that unlike traditional proteomics analyses, measured peptide intensities in LiP samples cannot be used to infer protein abundances, and each peptide should be treated as an independent measurement.[3] More interestingly, it is noted that 5 proteins, including PLMN, CO3, APOA1, HEMO and KV230, exhibited increased levels in the AD group compared to those in the control group within trypsin group and remained consistent with the change of their conformotypic peptides in the LiP group. Although further validation of the biological relevance between 5 proteins and their conformotypic peptides is needed, these observations potentially indicate that these specific proteins and their conformotypic peptides respectively act as potential candidate conformational biomarkers for AD condition at the protein and peptide level, which is

helpful to provide deeper understanding of their alterations in biological activities during AD progression.

Age and gender are regarded as primary risk factors for AD, though the specific pathogenic mechanisms of how age and gender affect AD-susceptibility are still unclear.[36, 37] Due to small sample size and close range of age in our participants, we did not find age related protein conformational changes between the AD and the control group in our current cohort. When correlating our results with the gender of the patients, we observed that 4 proteins including FA12 (Figure S5A), VWF (Figure S5B), APOA (Figure S5C) and HGFA (Figure S5D) showed significant changes in female samples between the AD and the control samples, while CBPN (Figure S5E) showed significant change in male samples between the AD and the control samples. In addition, elevated levels of VWF were observed in female serum samples of the AD patients compared to the control samples, these findings are consistent with a previous study, where elevated levels of VWF were observed in the sera of mild AD patients compared to controls.[38] Overall, these findings provide new insights into potential signaling pathways that may lead to higher incidence of AD in female than in male.

Gene ontology analysis of proteins changing proteolytic patterns in AD and control serum samples

For 23 proteins undergoing structural changes, the most common Gene Ontology terms were cellular anatomical entity, binding, catalytic activity, metabolic process, cellular process, and biological regulation (Figure S6). A KEGG pathway analysis revealed that the top-scoring pathway was complement and coagulation cascades (FDR-adjusted q-value, 3.04×10^{-12}), with 9 proteins (PLMN, FA12, C1R, CO3, CO9, C4BPA, VWF, PROS and CFAH) included in this pathway (Figure S7). Given the fact that complement proteins are associated with plaques and tangles in AD[39, 40] and three complement proteins (CO3, CO9 and C4BPA) are found to participate in this top-scoring pathway, we predict that this enriched pathway may provide key insight into the role of detected complement proteins in AD. Moreover, the disease terms enrichment analysis revealed that four proteins, including APOA1, APOA4, C1R and APOA, were related to AD progression. Taken together, these results demonstrate that the detected proteins undergoing structural changes are potentially involved in the pathogenesis and progression of AD.

Coverage comparative analysis of dysregulated proteins in the LiP group and trypsin group

To discover valuable molecular targets for AD at the protein level, we cross-validated the coverage of dysregulated proteins with significant changes (p-value < 0.05) in AD and control serum samples between LiP group and trypsin group. As shown in Venn diagram (Figure 5A), a total of 11 and 18 dysregulated proteins were discovered in LiP group and trypsin group, respectively. 4 proteins (including FBLN3 (Figure 5B), C1QA (Figure 5C), HPTR (Figure 5D) and FA12 (Figure 5E)) were shared between the LiP group and the trypsin group, presenting upregulated levels in the AD serum samples compared to that in the control serum samples. For these 4 shared proteins, FBLN3 is codified by the gene EFEMP1, which is an extracellular glycoprotein broadly distributed throughout

the body.[41] Previous study reported that FBLN3 was an amyloidogenic protein, causing systemic venous amyloidosis frequently found in the elderly population.[42] C1QA is one of the subunits of C1Q, which is the main protein of classical complement cascade.[43] Also, as one of the complement system members, C1QA belongs to the AD pathway and is related to amyloid-beta binding.[44] HPTR, as a primate-specific plasma protein, is associated with apolipoprotein L-I (apoL-I)-containing high-density lipoprotein (HDL).[45] Different studies from human, animal models, and bioengineered arteries confirmed that HDL protects against cerebrovascular dysfunction in AD.[46–48] FA12 is a serum glycoprotein that participates in misfolded protein binding, but no direct evidence as of a specific role for FA12 in AD has been reported.

Conclusively, our data further corroborated that several proteins (CO3, CO9, C4BPA, and C1QA) related to the complement system have been enriched either in KEGG pathway analyses or in comparative analysis of dysregulated proteins between LiP group and trypsin group, these proteins displayed elevated levels in AD patients compared to the controls. These findings are in good agreement with previous studies, which revealed that complement system dysregulation contributed to the pathogenesis of AD[49] and complement protein showed elevated expression levels in the AD brain samples.[40, 50] Although the underlying molecular mechanism of these complement proteins in AD remains to be explored in larger cohort and more diverse studies, these results have indicated the high versatility of detected complement proteins for targeted molecular diagnosis of AD. Taken together, these findings will aid in the elucidation of the mechanisms of AD pathogenesis, especially in respect to complement proteins with structural alterations, such as CO3, CO9, and C4BPA. We are currently conducting a study with a larger cohort to further verify the potential role of complement proteins and new aggregation-prone proteins undergoing structural changes in AD using CSF and matched serum samples.

Conclusions

This study presents an effective analytical method that enabled high-throughput quantitation of protein structural changes in serum samples collected from AD patients and control donors. Through the application of this method for serum protein analysis, 23 proteins were found to undergo structural changes. Amongst these proteins, 7 proteins including CO3, CO9, C4BPA, APOA1, APOA4, C1R and APOA, exhibited a close relationship with AD. Furthermore, we found that several complement proteins undergoing conformational changes (such as CO3, CO9 and C4BPA) associated with AD pathogenesis exhibited elevated levels in AD group compared to the control group. Nonetheless, larger and more diverse cohorts are required in future studies to explore the underlying molecular mechanisms of these complement proteins and structural changes of other proteins in AD. Current results suggest that the established DiLeu-LiP-MS method provides a powerful tool for high-throughput quantitative analysis of protein structural alterations, which also shows great potential for in-depth quantitative analysis of protein structural changes in complex biological systems.

Supplementary Material

Refer to Web version on PubMed Central for supplementary material.

ACKNOWLEDGMENTS

This work was supported in part by NIH grants (R21AG065728, RF1AG052324, R01AG078794, R01DK071801, and P41GM108538). Some of the mass spectrometers were acquired using NIH shared instrument grants S10 OD028473, S10 RR029531, and S10 OD025084. L.F. was supported in part by the NIH Chemistry-Biology Interface Training Grant (T32 GM008505). H.L. and H.Z. thank the funding support for a Postdoctoral Career Development Award provided by the American Society for Mass Spectrometry. Henrik Z. is a Wallenberg Scholar supported by grants from the Swedish Research Council (#2018-02532), the European Research Council (#681712 and #101053962), Swedish State Support for Clinical Research (#ALFGBG-71320), the Alzheimer Drug Discovery Foundation (ADDF), USA (#201809-2016862), the AD Strategic Fund and the Alzheimer's Association (#ADSF-21-831376-C, #ADSF-21-831381-C and #ADSF-21-831377-C), the Bluefield Project, the Olav Thon Foundation, the Erling-Persson Family Foundation, Stiftelsen för Gamla Tjänarinnor, Hjärnfonden, Sweden (#FO2022-0270), the European Union's Horizon 2020 research and innovation programme under the Marie Skłodowska-Curie grant agreement No 860197 (MIRIADE), the European Union Joint Programme-Neurodegenerative Disease Research (JPND2021-00694), and the UK Dementia Research Institute at UCL (UKDRI-1003).

REFERENCES

1. Almeida ZL; Brito RMM Structure and Aggregation Mechanisms in Amyloids. Molecules 2020, 25. [PubMed: 33374573]
2. Feng Y; De Franceschi G; Kahraman A; Soste M; Melnik A; Boersema PJ; de Laureto PP; Nikolaev Y; Oliveira AP; Picotti P Global Analysis of Protein Structural Changes in Complex Proteomes. Nat. Biotechnol. 2014, 32, 1036–1044. [PubMed: 25218519]
3. Schopper S; Kahraman A; Leuenberger P; Feng Y; Piazza I; Muller O; Boersema PJ; Picotti P Measuring Protein Structural Changes on a Proteome-Wide Scale Using Limited Proteolysis-Coupled Mass Spectrometry. Nat. Protoc. 2017, 12, 2391–2410. [PubMed: 29072706]
4. Chiti F; Dobson CM Protein Misfolding, Functional Amyloid, and Human Disease. Annu. Rev. Biochem. 2006, 75, 333–366. [PubMed: 16756495]
5. Bai B, et al. Deep Multilayer Brain Proteomics Identifies Molecular Networks in Alzheimer's Disease Progression. Neuron 2020, 105, 975–991 e977. [PubMed: 31926610]
6. Bai B, et al. U1 Small Nuclear Ribonucleoprotein Complex and Rna Splicing Alterations in Alzheimer's Disease. Proc. Natl. Acad. Sci. U. S. A. 2013, 110, 16562–16567. [PubMed: 24023061]
7. Tena J; Tang X; Zhou Q; Harvey D; Barajas-Mendoza M; Jin LW; Maezawa I; Zivkovic AM; Lebrilla CB Glycosylation Alterations in Serum of Alzheimer's Disease Patients Show Widespread Changes in N-Glycosylation of Proteins Related to Immune Function, Inflammation, and Lipoprotein Metabolism. Alzheimers Dement. (Amst) 2022, 14, e12309. [PubMed: 35496372]
8. Bamberger C; Pankow S; Martinez-Bartolome S; Ma M; Diedrich J; Rissman RA; Yates JR 3rd. Protein Footprinting Via Covalent Protein Painting Reveals Structural Changes of the Proteome in Alzheimer's Disease. J. Proteome Res. 2021, 20, 2762–2771. [PubMed: 33872013]
9. Martin L; Latypova X; Terro F Post-Translational Modifications of Tau Protein: Implications for Alzheimer's Disease. Neurochem. Int. 2011, 58, 458–471. [PubMed: 21215781]
10. Wegmann S; Biernat J; Mandelkow E A Current View on Tau Protein Phosphorylation in Alzheimer's Disease. Curr. Opin. Neurobiol. 2021, 69, 131–138. [PubMed: 33892381]
11. Tseng JH; Xie L; Song S; Xie Y; Allen L; Ajit D; Hong JS; Chen X; Meeker RB; Cohen TJ The Deacetylase Hdac6 Mediates Endogenous Neuritic Tau Pathology. Cell Rep. 2017, 20, 2169–2183. [PubMed: 28854366]
12. Murphy MP; LeVine H 3rd. Alzheimer's Disease and the Amyloid-Beta Peptide. J. Alzheimer's Dis. 2010, 19, 311–323. [PubMed: 20061647]

13. Chen GF; Xu TH; Yan Y; Zhou YR; Jiang Y; Melcher K; Xu HE Amyloid Beta: Structure, Biology and Structure-Based Therapeutic Development. Acta Pharmacol. Sin 2017, 38, 1205–1235. [PubMed: 28713158]

14. Yee AA; Savchenko A; Ignachenko A; Lukin J; Xu XH; Skarina T; Evdokimova E; Liu CS; Semesi A; Guido V; Edwards AM; Arrowsmith CH Nmr and X-Ray Crystallography, Complementary Tools in Structural Proteomics of Small Proteins. J. Am. Chem. Soc. 2005, 127, 16512–16517. [PubMed: 16305238]

15. Heyduk T Measuring Protein Conformational Changes by Fret/Lret. Curr. Opin. Biotechnol. 2002, 13, 292–296. [PubMed: 12323348]

16. Sakakibara D; Sasaki A; Ikeya T; Hamatsu J; Hanashima T; Mishima M; Yoshimasu M; Hayashi N; Mikawa T; Walchli M; Smith BO; Shirakawa M; Guntert P; Ito Y Protein Structure Determination in Living Cells by in-Cell Nmr Spectroscopy. Nature 2009, 458, 102–105. [PubMed: 19262674]

17. Leuenberger P; Ganscha S; Kahraman A; Cappelletti V; Boersema PJ; von Mering C; Claassen M; Picotti P Cell-Wide Analysis of Protein Thermal Unfolding Reveals Determinants of Thermostability. Science 2017, 355. [PubMed: 28126774]

18. Geiger R; Rieckmann JC; Wolf T; Basso C; Feng Y; Fuhrer T; Kogadeeva M; Picotti P; Meissner F; Mann M; Zamboni N; Sallusto F; Lanzavecchia A L-Arginine Modulates T Cell Metabolism and Enhances Survival and Anti-Tumor Activity. Cell 2016, 167, 829–842 e813. [PubMed: 27745970]

19. Ankney JA; Muneer A; Chen X Relative and Absolute Quantitation in Mass Spectrometry-Based Proteomics. Annu. Rev. Anal. Chem. (Palo Alto Calif.) 2018, 11, 49–77. [PubMed: 29894226]

20. Yu C; Huszagh A; Viner R; Novitsky EJ; Rychnovsky SD; Huang L Developing a Multiplexed Quantitative Cross-Linking Mass Spectrometry Platform for Comparative Structural Analysis of Protein Complexes. Anal. Chem. 2016, 88, 10301–10308. [PubMed: 27626298]

21. Savitski MM; Mathieson T; Zinn N; Sweetman G; Doce C; Becher I; Pachl F; Kuster B; Bantscheff M Measuring and Managing Ratio Compression for Accurate Itraq/Tmt Quantification. J. Proteome Res. 2013, 12, 3586–3598. [PubMed: 23768245]

22. Frost DC; Greer T; Li L High-Resolution Enabled 12-Plex Dileu Isobaric Tags for Quantitative Proteomics. Anal. Chem. 2015, 87, 1646–1654. [PubMed: 25405479]

23. Frost DC; Feng Y; Li L 21-Plex Dileu Isobaric Tags for High-Throughput Quantitative Proteomics. Anal. Chem. 2020, 92, 8228–8234. [PubMed: 32401496]

24. Pan JX; Han J; Borchers CH; Konermann L Characterizing Short-Lived Protein Folding Intermediates by Top-Down Hydrogen Exchange Mass Spectrometry. Anal. Chem. 2010, 82, 8591–8597. [PubMed: 20849085]

25. Vahidi S; Stocks BB; Liaghati-Mobarhan Y; Konermann L Submillisecond Protein Folding Events Monitored by Rapid Mixing and Mass Spectrometry-Based Oxidative Labeling. Anal. Chem. 2013, 85, 8618–8625. [PubMed: 23841479]

26. Fojtik L; Fiala J; Pompach P; Chmelik J; Matousek V; Beier P; Kukacka Z; Novak P Fast Fluoroalkylation of Proteins Uncovers the Structure and Dynamics of Biological Macromolecules. J. Am. Chem. Soc. 2021, 143, 20670–20679. [PubMed: 34846870]

27. Baczek T; Kaliszan R Predictions of Peptides' Retention Times in Reversed-Phase Liquid Chromatography as a New Supportive Tool to Improve Protein Identification in Proteomics. Proteomics 2009, 9, 835–847. [PubMed: 19160394]

28. Kim SJ; Back SH; Koh JM; Yoo HJ Quantitative Determination of Major Platelet Activating Factors from Human Plasma. Anal. Bioanal. Chem. 2014, 406, 3111–3118. [PubMed: 24682147]

29. Barwick VJ Sources of Uncertainty in Gas Chromatography and High-Performance Liquid Chromatography. J. Chromatogr. A 1999, 849, 13–33.

30. Cox J; Hein MY; Luber CA; Paron I; Nagaraj N; Mann M Accurate Proteome-Wide Label-Free Quantification by Delayed Normalization and Maximal Peptide Ratio Extraction, Termed Maxlfq. Mol. Cell. Proteomics 2014, 13, 2513–2526. [PubMed: 24942700]

31. Wang X; Shen S; Rasam SS; Qu J Ms1 Ion Current-Based Quantitative Proteomics: A Promising Solution for Reliable Analysis of Large Biological Cohorts. Mass Spectrom. Rev. 2019, 38, 461–482. [PubMed: 30920002]

32. Mitra G Emerging Role of Mass Spectrometry-Based Structural Proteomics in Elucidating Intrinsic Disorder in Proteins. Proteomics 2021, 21, e2000011. [PubMed: 32959512]
33. Xiang F; Ye H; Chen R; Fu Q; Li LN,N-Dimethyl Leucines as Novel Isobaric Tandem Mass Tags for Quantitative Proteomics and Peptidomics. Anal. Chem. 2010, 82, 2817–2825. [PubMed: 20218596]
34. Yu K; Niu M; Wang H; Li Y; Wu Z; Zhang B; Haroutunian V; Peng J Global Profiling of Lysine Accessibility to Evaluate Protein Structure Changes in Alzheimer's Disease. J. Am. Soc. Mass. Spectrom. 2021, 32, 936–945. [PubMed: 33683887]
35. Malinovska L; Cappelletti V; Kohler D; Piazza I; Tsai TH; Pepelnjak M; Stalder P; Dorig C; Sesterhenn F; Elsasser F; Kralickova L; Beaton N; Reiter L; de Souza N; Vitek O; Picotti P Proteome-Wide Structural Changes Measured with Limited Proteolysis-Mass Spectrometry: An Advanced Protocol for High-Throughput Applications. Nat. Protoc. 2022.
36. Alkallas R; Fish L; Goodarzi H; Najafabadi HS Inference of Rna Decay Rate from Transcriptional Profiling Highlights the Regulatory Programs of Alzheimer's Disease. Nat. Commun. 2017, 8, 909. [PubMed: 29030541]
37. Vina J; Lloret A Why Women Have More Alzheimer's Disease Than Men: Gender and Mitochondrial Toxicity of Amyloid-Beta Peptide. J. Alzheimers Dis. 2010, 20 Suppl 2, S527–533. [PubMed: 20442496]
38. Hanas JS; Hocker JRS; Vannarath CA; Lerner MR; Blair SG; Lightfoot SA; Hanas RJ; Couch JR; Hershey LA Distinguishing Alzheimer's Disease Patients and Biochemical Phenotype Analysis Using a Novel Serum Profiling Platform: Potential Involvement of the Vwf/Adamts13 Axis. Brain Sci 2021, 11. [PubMed: 35053755]
39. Tenner AJ Complement-Mediated Events in Alzheimer's Disease: Mechanisms and Potential Therapeutic Targets. J. Immunol. 2020, 204, 306–315. [PubMed: 31907273]
40. Wyss-Coray T; Rogers J Inflammation in Alzheimer Disease-a Brief Review of the Basic Science and Clinical Literature. Cold Spring Harb. Perspect. Med. 2012, 2, a006346. [PubMed: 22315714]
41. Zhang Y; Marmorstein LY Focus on Molecules: Fibulin-3 (Efemp1). Exp. Eye Res. 2010, 90, 374–375. [PubMed: 19799900]
42. Tasaki M; Ueda M; Hoshii Y; Mizukami M; Matsumoto S; Nakamura M; Yamashita T; Ueda A; Misumi Y; Masuda T; Inoue Y; Torikai T; Nomura T; Tsuda Y; Kanenawa K; Isoguchi A; Okada M; Matsui H; Obayashi K; Ando Y A Novel Age-Related Venous Amyloidosis Derived from Egf-Containing Fibulin-Like Extracellular Matrix Protein 1. J. Pathol. 2019, 247, 444–455. [PubMed: 30565683]
43. Xu J; Zhou H; Xiang G Identification of Key Biomarkers and Pathways for Maintaining Cognitively Normal Brain Aging Based on Integrated Bioinformatics Analysis. Front. Aging Neurosci. 2022, 14, 833402. [PubMed: 35356296]
44. Kubota T; Maruyama S; Abe D; Tomita T; Morozumi T; Nakasone N; Saku T; Yoshie H Amyloid Beta (A4) Precursor Protein Expression in Human Periodontitis-Affected Gingival Tissues. Arch. Oral Biol. 2014, 59, 586–594. [PubMed: 24690593]
45. Nielsen MJ; Petersen SV; Jacobsen C; Oxvig C; Rees D; Moller HJ; Moestrup SK Haptoglobin-Related Protein Is a High-Affinity Hemoglobin-Binding Plasma Protein. Blood 2006, 108, 2846–2849. [PubMed: 16778136]
46. Button EB; Robert J; Caffrey TM; Fan J; Zhao W; Wellington CL Hdl from an Alzheimer's Disease Perspective. Curr. Opin. Lipidol. 2019, 30, 224–234. [PubMed: 30946049]
47. Robert J; Button EB; Yuen B; Gilmour M; Kang K; Bahrabadi A; Stukas S; Zhao W; Kulic I; Wellington CL Clearance of Beta-Amyloid Is Facilitated by Apolipoprotein E and Circulating High-Density Lipoproteins in Bioengineered Human Vessels. Elife 2017, 6.
48. Hong BV; Zheng J; Agus JK; Tang X; Lebrilla CB; Jin LW; Maezawa I; Erickson K; Harvey DJ; DeCarli CS; Mungas DM; Olichney JM; Farias ST; Zivkovic AM High-Density Lipoprotein Changes in Alzheimer's Disease Are Apoe Genotype-Specific. Biomedicines 2022, 10. [PubMed: 36672517]
49. Lee JD; Coulthard LG; Woodruff TM Complement Dysregulation in the Central Nervous System During Development and Disease. Semin. Immunol. 2019, 45, 101340. [PubMed: 31708347]

50. Bai B; Vanderwall D; Li Y; Wang X; Poudel S; Wang H; Dey KK; Chen PC; Yang K; Peng J Proteomic Landscape of Alzheimer's Disease: Novel Insights into Pathogenesis and Biomarker Discovery. Mol. Neurodegener. 2021, 16, 55. [PubMed: 34384464]

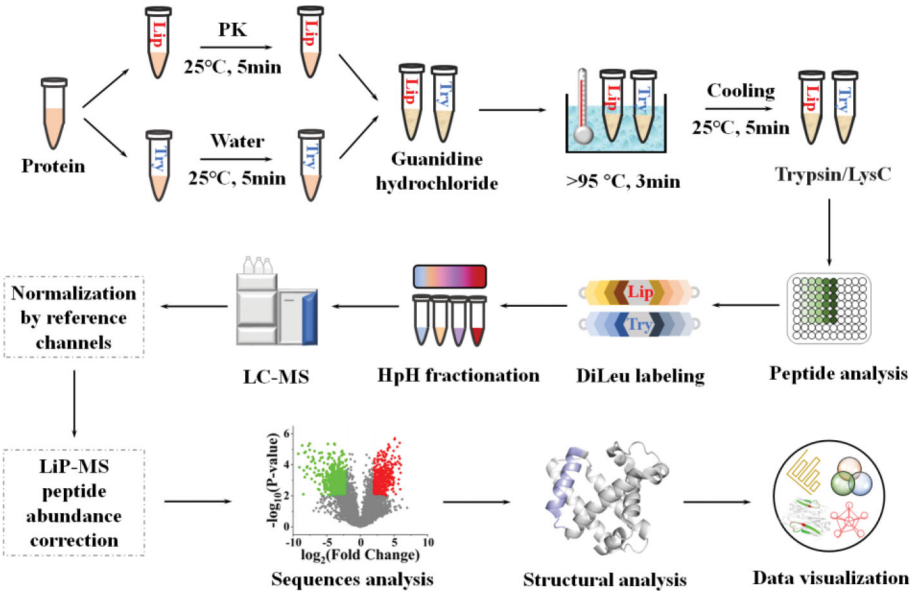

Figure 1.

The workflow of DiLeu-LiP-MS for high-throughput quantitation analysis of proteins undergoing structural changes.

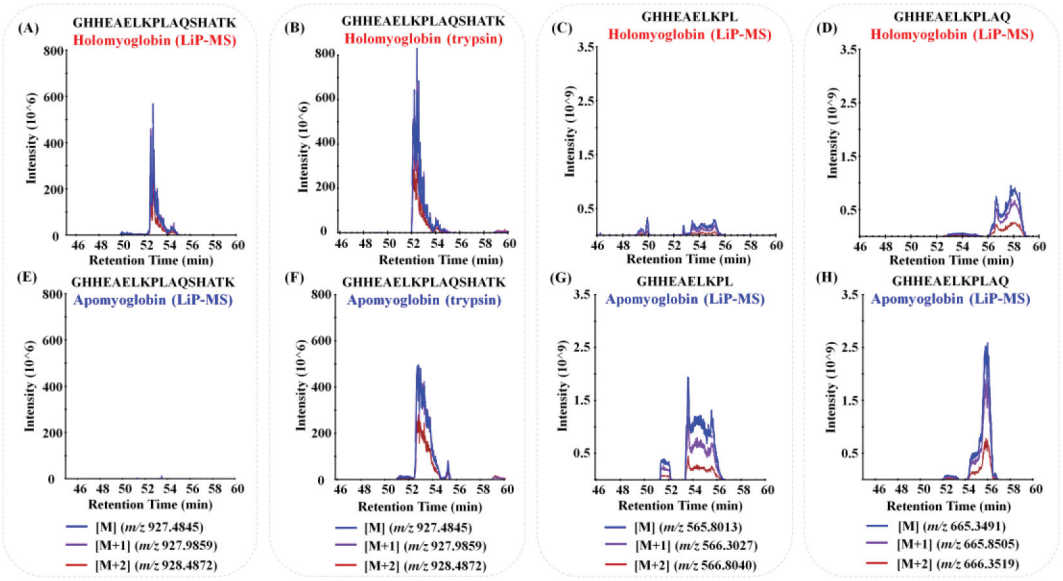

Figure 2.

Conformotypic peptides of holomyoglobin and apomyoglobin obtained from label-free LiP-MS quantitation. Fully tryptic peptide (GHHEAELKPLAQSHATK) intensity changes of holomyoglobin (A) and apomyoglobin (E) in LiP-MS group. Fully tryptic peptide (GHHEAELKPLAQSHATK) intensity changes of holomyoglobin (B) and apomyoglobin (F) in trypsin group. Half-tryptic peptide (GHHEAELKPL) intensity changes of holomyoglobin (C) and apomyoglobin (G) in LiP-MS group. Half-tryptic peptide (GHHEAELKPLAQ) intensity changes of holomyoglobin (D) and apomyoglobin (H) in LiP-MS group.

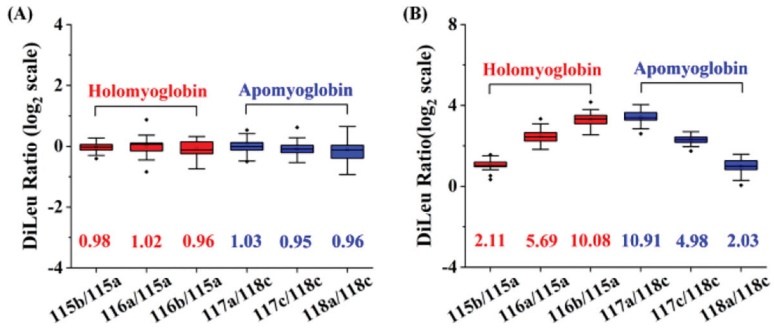

Figure 3.

Evaluation of quantitative accuracy and dynamic range of 8-plex DiLeu-LiP-MS in protein structural changes. The results of 8-plex DiLeu-labeled holomyoglobin and apomyoglobin peptides in 1:1:1:1:1:1:1:1 ratios (A) and in 1:2:5:10:10:5:2:1 ratios (B) are shown in the box plots.

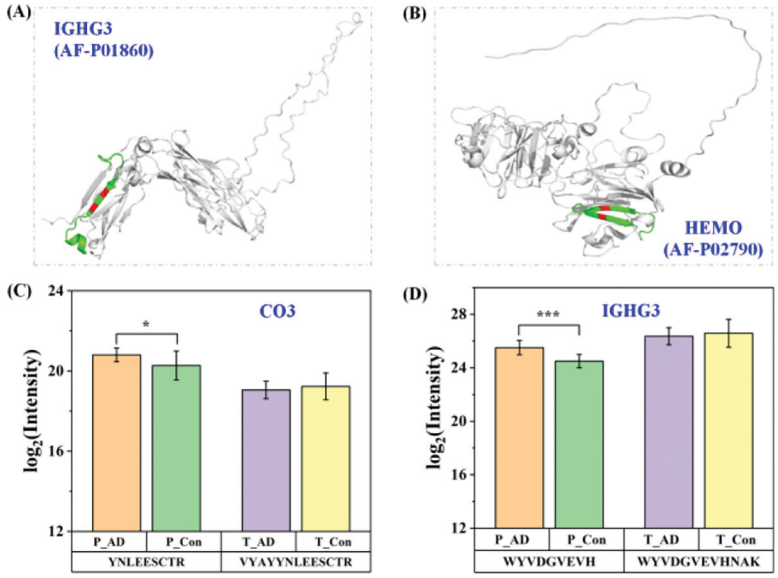

Figure 4.

Fully tryptic peptides of (A) IGHG3 and (B) HEMO with more than one LiP cleavage site (green color indicated the fully tryptic peptides, red color indicated the LiP cleavage site). Relative quantitation of conformotypic peptides mapping to their proteins undergoing a structural change, including (C) CO3 and (D) IGHG3. P_AD and P_Con respectively indicated AD and control samples in the LiP group, T_AD and T_Con respectively indicated AD and control samples in trypsin group, graphed as mean ± standard deviation (n = 11 in AD per group, n = 10 in control group). Significant difference was determined by a two-tailed t test (*$p < 0.05$, and ***$p < 0.001$).

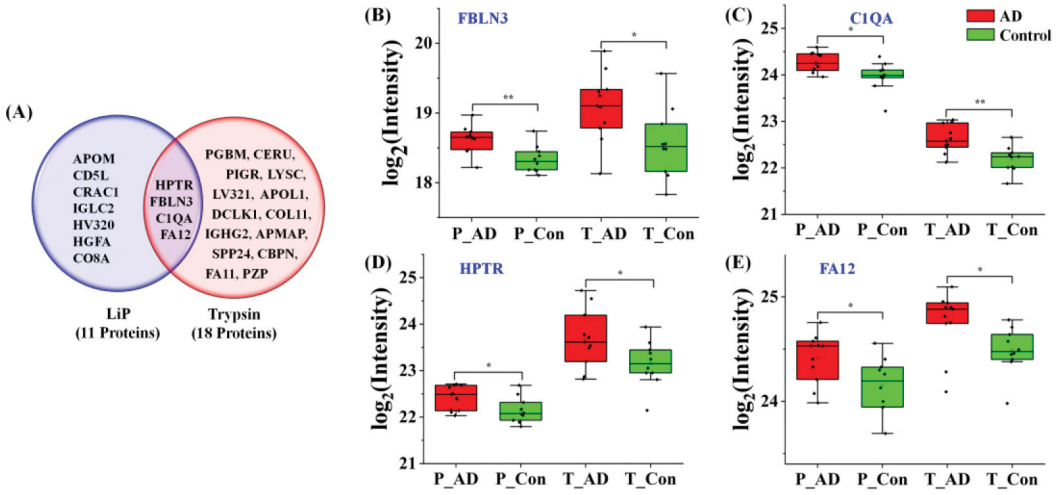

Figure 5.

(A) Venn diagram indicated coverage of significantly changed proteins in AD and control serum samples between LiP group (purple circle) and trypsin group (red circle). Box plots showed expression levels of 4 shared significantly changed proteins (B) FBNL3, (C) C1QA, (D) HPTR and (E) FA12 in AD and control serum samples between LiP group and trypsin group. P indicated LiP group, T indicated trypsin group. Significant difference was determined by a two-tailed t test (*$p < 0.05$, and **$p < 0.01$).